SCIENTIFIC REPORTS

OPEN

Emergence of Multiple Superconducting Phases in $(NH_3)_yM_xFeSe$ (M: Na and Li)

Received: 17 March 2015
Accepted: 10 July 2015
Published: 04 August 2015

Lu Zheng[1], Xiao Miao[1], Yusuke Sakai[1], Masanari Izumi[1], Hidenori Goto[1], Saki Nishiyama[1], Eri Uesugi[1], Yuichi Kasahara[2], Yoshihiro Iwasa[2] & Yoshihiro Kubozono[1,3]

We previously discovered multiple superconducting phases in the ammoniated Na-doped FeSe material, $(NH_3)_yNa_xFeSe$. To clarify the origin of the multiple superconducting phases, the variation of T_c was fully investigated as a function of x in $(NH_3)_yNa_xFeSe$. The 32 K superconducting phase is mainly produced in the low-x region below 0.4, while only a single phase is observed at x = 1.1, with T_c = 45 K, showing that the T_c depends significantly on x, but it changes discontinuously with x. The crystal structure of $(NH_3)_yNa_xFeSe$ does not change as x increases up to 1.1, *i.e.*, the space group of $I4/mmm$. The lattice constants, *a* and *c*, of the low-T_c phase (T_c = 32.5 K) are 3.9120(9) and 14.145(8) Å, respectively, while *a* = 3.8266(7) Å and *c* = 17.565(9) Å for the high-T_c phase (~46 K). The *c* increases in the high T_c phase, implying that the T_c is directly related to *c*. In $(NH_3)_yLi_xFeSe$ material, the T_c varies continuously within the range of 39 to 44 K with changing x. Thus, the behavior of T_c is different from that of $(NH_3)_yNa_xFeSe$. The difference may be due to the difference in the sites that the Na and Li occupy.

Any strategy for increasing the superconducting transition temperature (T_c) in metal-doped FeSe is a most exciting research subject, because the T_c can be effectively increased in metal-doped FeSe using a variety of methods such as ammoniation[1–5], pressure application[6] and solvent intercalation[7]; FeSe corresponds to PbO-type FeSe, *i.e.*, β-FeSe. The highest T_c reported in bulk superconductors of metal-doped FeSe is ~50 K, as recorded in $Tl_{0.6}Rb_{0.4}Fe_{1.67}Se_2$ and $K_{0.8}Fe_{1.7}Se_2$[6] under high pressure; through this paper, the chemical representation of $(NH_3)_yM_xFeSe$ is used instead of $(NH_3)_yM_{x'}Fe_2Se_2$. Our representation refers to the primitive basis of the crystal. Therefore, x = x'/2. At ambient pressure, the highest T_c in metal-doped FeSe materials is 46 K for $(NH_3)_yNa_{0.5}FeSe$[1]. In metal-doped FeSe, the T_c increases with an increase in the lattice constant *c*, or the plane spacing between FeSe layers. The insertion of NH_3 molecules or ammoniated metal coordinates between the FeSe layers can expand the *c*. The ammoniation and metal intercalation in FeSe (or the formation of $(NH_3)_yM_xFeSe$) can be simultaneously achieved by dissolving metal and FeSe in liquid NH_3 at low temperature. Recently, we succeeded in synthesizing $(NH_3)_yM_xFeSe_{0.5}Te_{0.5}$ using the liquid NH_3 technique[8], and found that the T_c of $(NH_3)_yNa_xFeSe_{0.5}Te_{0.5}$ is lower than that of the corresponding FeSe materials. Thus, the liquid NH_3 technique is applicable to the intercalation of metal atoms into various $FeSe_{1-z}Te_z$ ($0.0 \leq z \leq 1.0$). The chemical doping of metal atoms and NH_3 or ammoniated metal coordinates provides the advantage of expanding the two-dimensional (2D) layer spacing, which may contribute to an improved T_c.

Recently, the presence of multiple superconducting phases has been clarified in $(NH_3)_yK_xFeSe$[4] and $(NH_3)_yNa_xFeSe$[8]. In $(NH_3)_yK_xFeSe$, a high-T_c phase (T_c = 44 K) was discovered in addition to the low-T_c phase (T_c = 30 K)[4]. The x-dependence of T_c was found to involve a discontinuous change in T_c; the high-T_c phase was observed with low x values, and the low-T_c phase found with high x values. The T_c was

[1]Research Laboratory for Surface Science, Okayama University, Okayama 700-8530, Japan. [2]Department of Applied physics, The University of Tokyo, Tokyo 113-8564, Japan. [3]Research Centre of New Functional Materials for Energy Production, Storage and Transport, Okayama University, Okayama 700-8530, Japan. Correspondence and requests for materials should be addressed to Y.K. (email: kubozono@cc.okayama-u.ac.jp)

correlated with *c*, *i.e.*, a smaller *c* resulted in a lower T_c. Discovering the presence of multiple phases is significant because of the possibility that a phase with even higher T_c might be found, even in metal-doped FeSe compositions previously examined. This makes the search for multiple superconducting phases in other FeSe materials important and exciting.

As described above, we recently discovered a new superconducting phase (low-T_c phase: $T_c = 31.5$ K[8]) in addition to the high-T_c phase ($T_c = 46$ K[1]) reported previously in $(NH_3)_yNa_xFeSe$. However, a systematic study on the origin of the different superconducting phases has not yet been performed, although a difference in *c* was found for the two phases. Also, the relationship between T_c and x has not yet been investigated in $(NH_3)_yNa_xFeSe$. Here we systematically study the variation of T_c as a function of x in $(NH_3)_yNa_xFeSe$. Furthermore, the lattice constants were determined for the superconducting phases realized at different x's to clarify the correlation between T_c and lattice constants. The variation of T_c in $(NH_3)_yLi_xFeSe$ was also investigated as a function of x. Some interesting points to be clarified are as follows: (1) the presence of multiple superconducting phases, (2) the discontinuous or continuous variation of T_c, and (3) the origin of the variation of T_c. In this study, the superconducting phases were identified in the $(NH_3)_yNa_xFeSe$ and $(NH_3)_yLi_xFeSe$ samples, so that the answers were provided for the above important points.

Results

Multiple superconducting phases in $(NH_3)_yNa_xFeSe$. Figure 1(a),(b) show the *M* / *H* curves of typical low-T_c and high-T_c phases of $(NH_3)_yNa_xFeSe$, respectively. In the former sample nominal x = 0.1, and in the latter nominal x = 1.0. These samples each contain a 'single phase', either low-T_c or high-T_c; actually a trace of non-doped β-FeSe ($T_c = 8$ K) is found in Fig. 1(a). The T_c^{onset} and T_c were determined to be 35 and 32.5 K from *M* / *H* curves at ZFC for the low-T_c phase (Fig. 1(a)), while the T_c^{onset} and T_c were 47 and 46 K at ZFC for the high-T_c phase (Fig. 1(b)). How the T_c was determined is shown in the insets of Fig. 1(a),(b). The shielding fractions at 10 K were evaluated to be 30.5% for the low-T_c phase and 26% for the high T_c phase.

Figure 1(c),(d) show the XRD patterns of the low-T_c and high-T_c phases of $(NH_3)_yNa_xFeSe$, respectively. The T_c^{onset} and T_c for the former sample (nominal x = 0.2) were determined to be 35 and 32.5 K, respectively, from the *M* / *H* curve (not shown) in ZFC mode, and the shielding fraction at 10 K was 18%. No high-T_c phase was observed in this sample, but non-doped β-FeSe was included in the sample. The latter sample (nominal x = 1.0) is the same as that providing the *M* / *H* curve shown in Fig. 1(b); no low-T_c phase was observed in the *M* / *H vs. T* curve of this sample.

The *a* and *c* were determined to be 3.9120(9) Å and 14.145(8) Å, respectively, for the low-T_c phase (Fig. 1(c)), while the *a* and *c* were 3.8266(7) Å and 17.565(9) Å respectively, for the high-T_c phase (Fig. 1(d)). The values of *a* and *c* were determined using LeBail fitting under the space group of *I*4/mmm, suggesting no change of crystal structure between the low-T_c and high-T_c phases. The *a* and *c* values for both the phases were close to those reported previously by our group ($a = 3.891(2)$ Å and $c = 14.269(4)$ Å for the low-T_c phase; $a = 3.8275(6)$ Å and $c = 17.579(5)$ Å, for the high-T_c phase)[9]. Furthermore, the *a* and *c* for the high-T_c phase determined in this study are also consistent with those reported by Ying *et al.* ($a = 3.7846(4)$ Å and $c = 17.432(1)$ Å)[1]. From the lattice constants, it has been concluded that a larger *c* produces a higher T_c. This conclusion is supported by the relation between T_c and *c* found in $(NH_3)_yM_xFeSe$ materials with various M[5].

X dependence of superconductivity in $(NH_3)_yNa_xFeSe$. To clarify the exact stoichiometry of $(NH_3)_yNa_xFeSe$ samples prepared in this study, the energy dispersive X-ray (EDX) spectroscopy was measured. To confirm the accuracy and precision of x determined by EDX, the x was determined for a reference sample, NaCl (purity = 99.0%). The EDX of NaCl showed $Na_{1.0(1)}Cl$, which means that the EDX can provide the x value with high accuracy and precision. The typical EDX spectra of the samples containing low-T_c and high-T_c phases are shown in Figures S1 and S2 of Supplementary Information. The exact stoichiometric composition of the $(NH_3)_yNa_{0.1}FeSe$ sample (nominal composition of Na = 0.1) with $T_c = 33.6$ K (low-T_c phase) was expressed as '$(NH_3)_yNa_{0.17(3)}FeSe$', while the exact stoichiometric composition of the $(NH_3)_yNa_{1.0}FeSe$ sample (nominal composition of Na = 1.0) with $T_c = 45.1$ K (high-T_c phase) was '$(NH_3)_yNa_{1.1(1)}FeSe$'. These results show the consistency between the nominal and actual stoichiometry. However, the stoichiometric compositions of some samples determined from EDX spectra deviated within 0.3 from the nominal compositions, suggesting the difficulty in making the target material using liquid reaction method. Therefore, we use the x values determined from the EDX spectroscopy for x dependence of T_c and *c* in $(NH_3)_yNa_xFeSe$ samples. Notably, the exact amounts of NH_3 contained in the samples could not be determined from EDX. Furthermore, we can comment on Fe vacancy. The EDX provided the chemical composition of Fe as 0.80(5) for $(NH_3)_yNa_{0.17(3)}FeSe$, *i.e.*, it can be expressed as '$(NH_3)_yNa_{0.17(3)}Fe_{0.80(5)}Se$' if considering the Fe vacancy. The stoichiometry of Fe was 0.70–0.84 in all samples, suggesting that ~75% of 4*d* site is occupied by Fe atom. Through this paper, we do not show the exact stoichiometry of Fe for all samples because it does not change as a function of x, *i.e.*, it does not relate to the change of lattice parameters and T_c.

The T_c's of all $(NH_3)_yNa_xFeSe$ samples prepared in this study are plotted as a function of x, as shown in Fig. 2(a); the x is determined from EDX spectroscopy. In the low-x region below 0.4, the low-T_c phase ($T_c = 32$ K) predominates in the samples, and all the samples substantially contain either the low-T_c

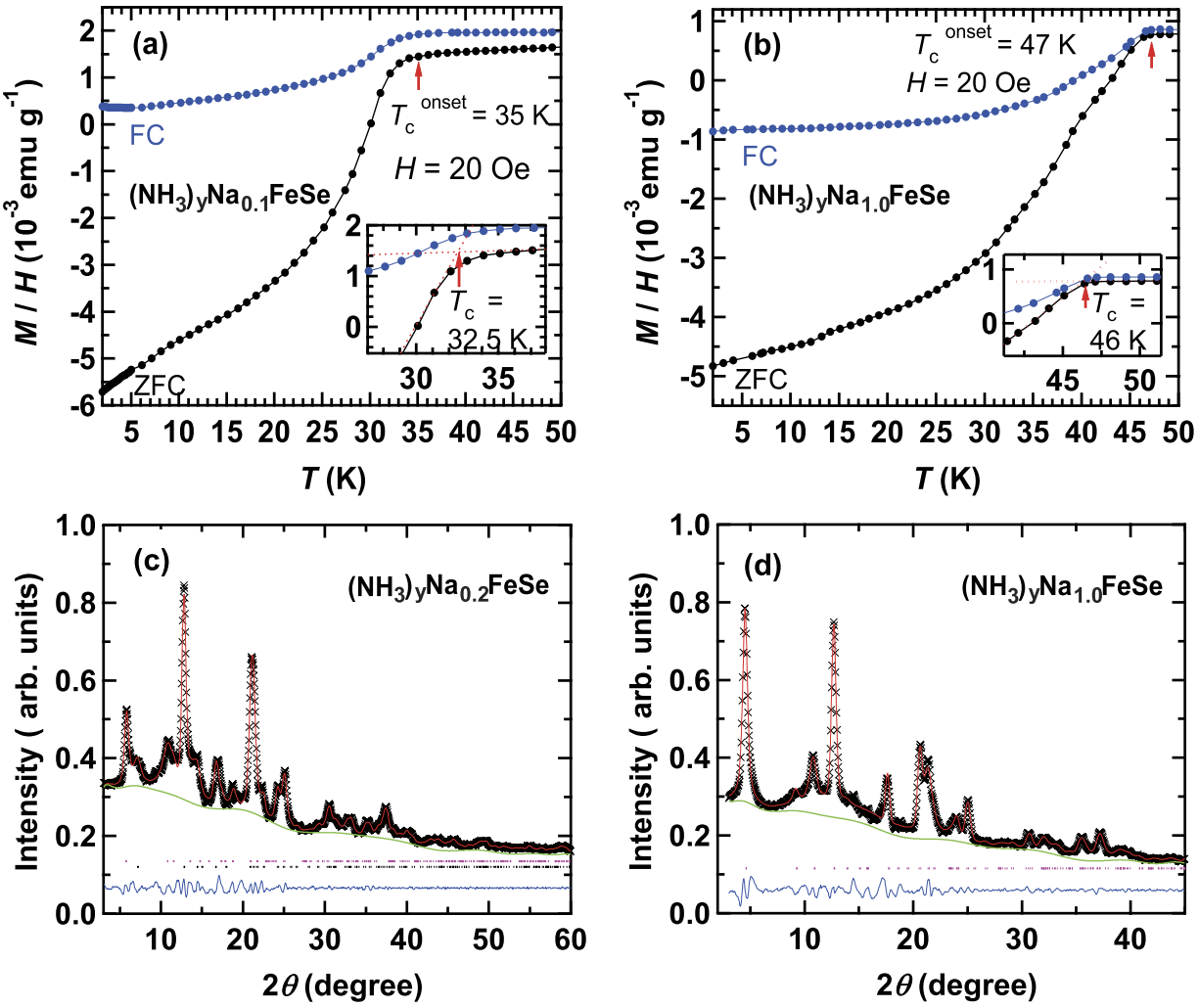

Figure 1. *M* / *H vs. T* plots of **(a)** $(NH_3)_yNa_{0.1}FeSe$ (low-T_c phase) and (b) $(NH_3)_yNa_{1.0}FeSe$ (high-T_c phase) in ZFC and FC modes ($H = 20$ Oe). Insets in (**a**) and (**b**) show the method used to determine T_c. XRD patterns of (**c**) $(NH_3)_yNa_{0.2}FeSe$ (low-T_c phase) and (**d**) $(NH_3)_yNa_{1.0}FeSe$ (high-T_c phase); 'x' marks correspond to the experimental XRD patterns. Red and green lines refer to calculated patterns (LeBail fitting) and background, respectively. Ticks refer to the peak positions predicted. In (**c**), two phases ($(NH_3)_yNa_{0.2}FeSe$ and β-FeSe) are used in LeBail fitting, while in (**d**), a single phase ($(NH_3)_yNa_{1.0}FeSe$) is used.

($T_c = 32$ K) or high-T_c ($T_c \sim 45$ K) phase, *i.e.*, a predominant phase exists in each sample. The T_c of the low-T_c phase does not change throughout the entire x region. As seen from Fig. 2(a), the high-T_c phase tends to be produced in the high-x region. The T_c of the high-T_c phase does not change with an increase in x, suggesting that $(NH_3)_yNa_xFeSe$ does not show solid solution-like behavior (continuous change of T_c), but discontinuous superconducting phases. Only a phase exhibiting high T_c (~45 K) is produced at $x = 1.1$ in $(NH_3)_yNa_xFeSe$. At $x = 0.5$–0.9, either low-T_c or high-T_c phase is observed. These results show that the higher T_c is realized in the samples with higher x values. In other words, the T_c can be controlled by changing the proportion of Na (or x) in $(NH_3)_yNa_xFeSe$. Here we briefly comment the amount of NH_3. In this study, the NH_3 amount was detected for only the low-T_c phase by the mass difference before and after the ammoniation. The y value of the low-T_c phase was scattered in 0.2–0.6. Nevertheless, the presence of NH_3 was evidenced for the low-T_c phase, which is fully discussed in the **Discussion** section.

The XRD patterns of $(NH_3)_yNa_xFeSe$ at the x values of 0.3, 0.5 and 1.1 are shown in Fig. 2(b); the x values refer to those determined from EDX. A similar XRD pattern is observed in all x values, *i.e.*, the same crystal structure (*I*4/mmm). The expanded XRD patterns are shown in Fig. 2(c), exhibiting a pronounced 002 peak at $2\theta = 5.80°$ and a very weak 002 peak at $2\theta = 4.50°$ for $x = 0.3$ and only a peak at $2\theta = 4.50°$ for $x = 1.1$. This means that *c* is greater when $x = 1.1$ than the main phase (low-T_c phase) at $x = 0.3$. At $x = 0.5$, two peaks (intense and weak peaks) are observed, at $2\theta = 5.80°$ and $2\theta = 4.50°$, respectively, suggesting that two phases coexist in one sample in this x region but the high-T_c phase's

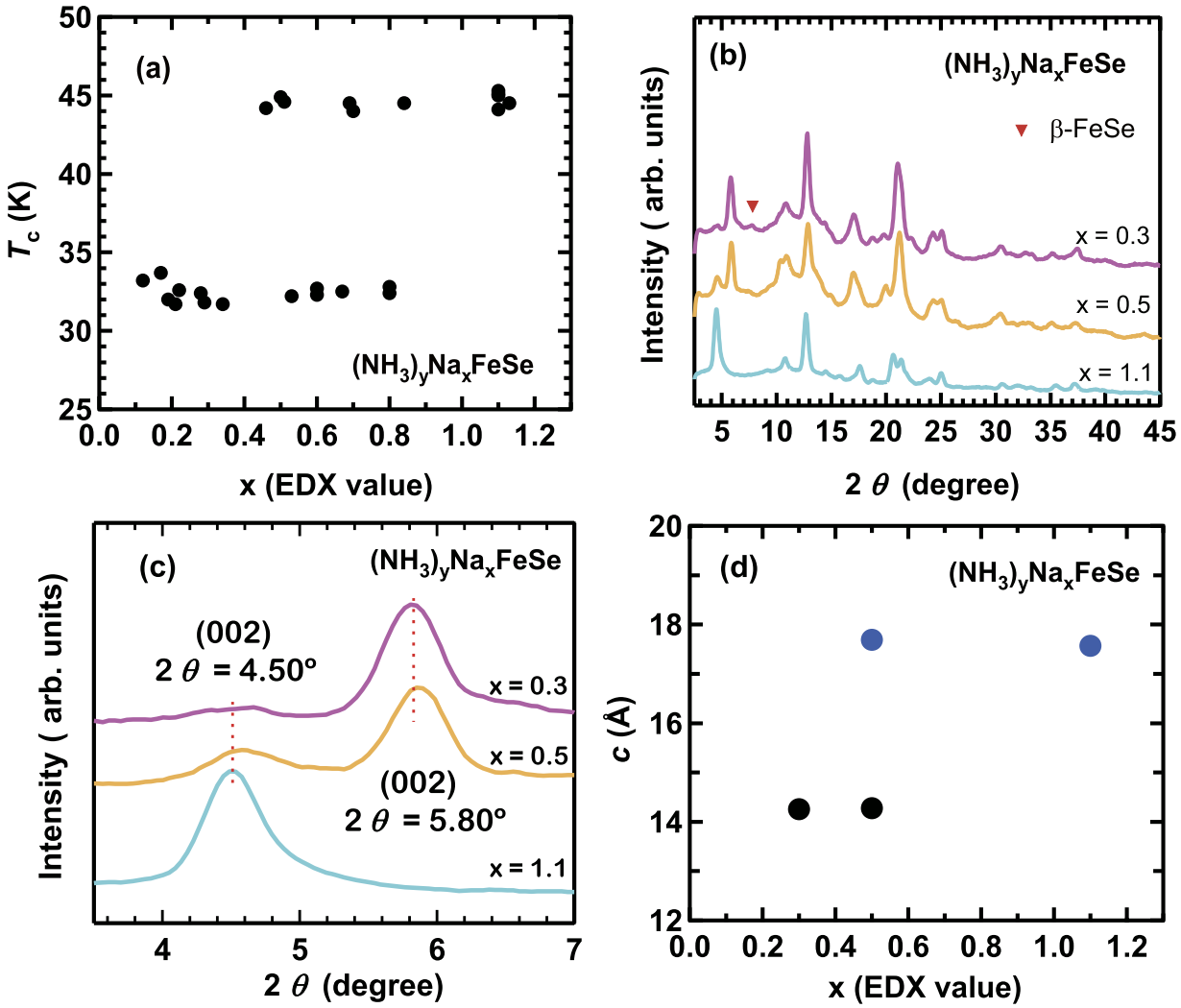

Figure 2. (**a**) T_c *vs.* x plots for $(NH_3)_yNa_xFeSe$. x is determined from EDX spectra of the samples. (**b**) XRD patterns of $(NH_3)_yNa_xFeSe$ at x = 0.3, 0.5 and 1.1. (**c**) XRD peaks ascribable to 002 reflection of $(NH_3)_yNa_xFeSe$ at x = 0.3, 0.5 and 1.1. (**d**) *c* vs. x plots in $(NH_3)_yNa_xFeSe$. Solid black and blue circles refer to low-T_c and high-T_c phases, respectively.

peak is small. Thus, the XRD peak discontinuously shifts from $2\theta = 5.80°$ to $2\theta = 4.50°$, which implies that only two structural phases exist, even when the x value changes. In other words, a solid-solution like structure does not appear in the $(NH_3)_yNa_xFeSe$ material. The x dependence of *c* determined by a LeBail fitting for the XRD patterns is shown in Fig. 2(d), which provides a constant *c* in the low T_c-phase for x = 0.3 and 0.5 and a constant *c* in the high-T_c phase for x = 0.5 and 1.1. The *a* is constant in the whole x values, indicating that the observed variation in T_c is not related to *a*, as seen from Fig. S3 of Supplementary Information.

X dependence of superconductivity in $(NH_3)_yLi_xFeSe$. Figure 3(a) shows the *M* / *H* curves in ZFC and FC modes for $(NH_3)_yLi_xFeSe$ at x = 0.1. Notably, the x value is nominal because EDX cannot provide the exact stoichiometric composition of Li; the detection of Li peak was impossible in our EDX spectrometer because of the confined energy range. The T_c^{onset} and T_c were determined to be 42 and 39.5 K from *M* / *H* curve at ZFC. The shielding fraction was evaluated to be 25.5% at 10 K. The *M* / *H vs. T* curve shows that this sample contains only a single superconducting phase. We made the $(NH_3)_yLi_xFeSe$ samples (x = 0.1 to 0.9), and when their *M* / *H* curves were measured, they showed only a single superconducting phase. The average T_c, $<T_c>$, is plotted with the estimated standard deviation (esd) as a function of x in Fig. 3(b); the $<T_c>$ was evaluated from three samples. The $<T_c>$ *vs.* x plot shows a continuous variation. It slowly increases with increasing x up to 0.7; $<T_c> = 43.5$ K, and decreases slightly from 0.7. The maximum T_c (= 44 K) is observed at x = 0.7. However, the variation is at most 5 K. The dome-like behavior in T_c *vs.* x plot shown in Fig. 3(b) was not observed in $(NH_3)_yNa_xFeSe$. Thus, it has

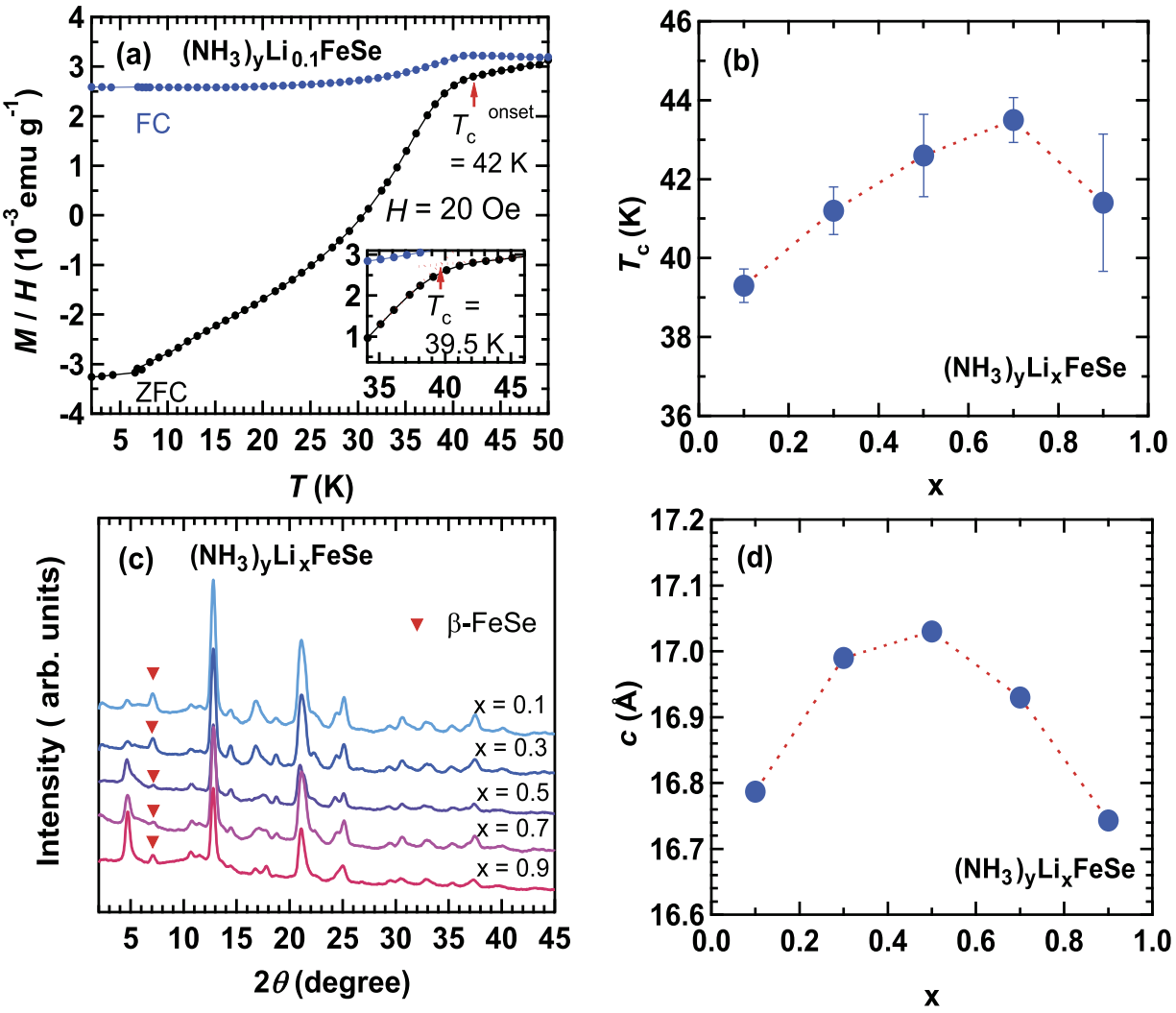

Figure 3. (**a**) *M* / *H vs. T* plots of $(NH_3)_yLi_{0.1}FeSe$ in ZFC and FC modes ($H = 20$ Oe). Inset in (a) shows the method used to determine T_c. (**b**) T_c *vs.* x plot in $(NH_3)_yLi_xFeSe$. (**c**) XRD patterns of $(NH_3)_yLi_xFeSe$ at $x = 0.1$ to 0.9. (**d**) *c* vs. x plots in $(NH_3)_yLi_xFeSe$; x is nominal value.

been concluded that the behavior of T_c versus x in $(NH_3)_yM_xFeSe$ is completely different depending on whether M = Na or Li. Although the nominal x was used in the plot of $(NH_3)_yLi_xFeSe$, this conclusion should be reliable. The dome-like behavior of T_c – x (Fig. 3b) must be validated by the T_c – x plot using actual x value which may be determined by neutron diffraction.

Figure 3(c) shows the XRD patterns of $(NH_3)_yLi_xFeSe$ ($x = 0.1$ to 0.9); x is the nominal values. The XRD patterns of $(NH_3)_yLi_xFeSe$ are the same in all x regions. The XRD patterns could be reproduced with two phases of $(NH_3)_yLi_xFeSe$ and small amounts of β-FeSe. The *c* value, determined using LeBail fitting, gradually increases with increasing x up to 0.5, and decreases monotonically, as seen from Fig. 3(d); the maximum *c* (= 17.03(2) Å) is observed at $x = 0.5$; the typical LeBail fitting for the XRD pattern is shown in Figure S4 of Supplementary Information. The results show clearly that T_c is correlated with *c*. Compared with *c* value, *a* value is almost constant (see Figure S5 of Supplementary Information). As in $(NH_3)_yNa_xFeSe$, the larger *c* provides the higher T_c in $(NH_3)_yLi_xFeSe$, but the *c* changes continuously in $(NH_3)_yLi_xFeSe$, in contrast to the *c vs.* x plot in $(NH_3)_yNa_xFeSe$. Thus, solid-solution like behavior is observed in both T_c and *c* in $(NH_3)_yLi_xFeSe$.

Discussion

Here we must consider why *c* is different in the low-T_c and high-T_c phases. As shown for $(NH_3)_yLi_xFeSe$, with a T_c as high as 43 K, the Li atoms occupy an off-center position in the *I*4/mmm lattice (Fig. 4(a))[2]. Specifically, the Li atoms occupy the 4*c* site (0,1/2,0) and 2*b* site (0,0,1/2). The T_c (= 43 K)[2] and the *c* (= 16.5266(9) Å)[2] of $(NH_3)_yLi_xFeSe$ are close to those of the high-T_c phase ($T_c = 46$ K and $c = 17.565(9)$ Å) of $(NH_3)_yNa_xFeSe$. The difference in *c*, Δ*c*, between $(NH_3)_yLi_xFeSe$ and the high-T_c phase of $(NH_3)_yNa_xFeSe$ may be due to the different ionic radii of Li and Na and consequent differences in local structure around

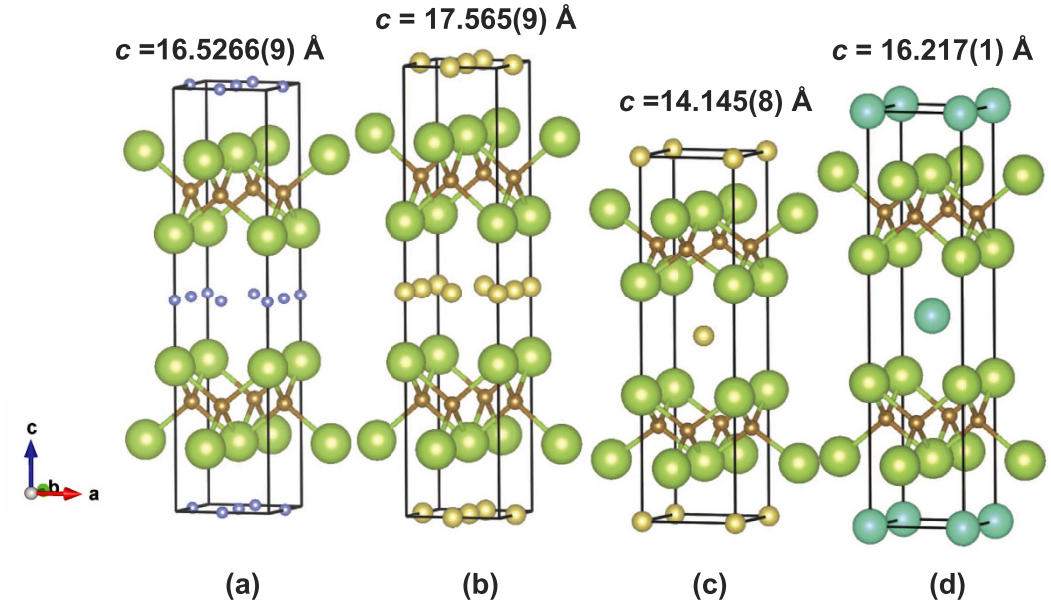

Figure 4. Crystal structures determined for (**a**) $(NH_3)_yLi_xFeSe$ (ref. 2) and (d) $(NH_3)_yCs_xFeSe$ (ref. 5), and the structure suggested for (**b**) high-T_c phase and (**c**) low-T_c phase of $(NH_3)_yNa_xFeSe$. Green, brown, blue, yellow, and dark green balls refer to Se, Fe, Li, Na and Cs, respectively. Ball sizes reflect relative ionic radii. N and H are not shown. All schematic structures are drawn by ourselves based on the crystal structures determined for $(NH_3)_yLi_xFeSe$ (ref. 2) and $(NH_3)_yCs_xFeSe$ (ref. 5), and those of high-T_c and low-T_c phases of $(NH_3)_yNa_xFeSe$ are drawn by ourselves using atomic coordinates of $(NH_3)_yLi_xFeSe$ (ref. 2) and $(NH_3)_yCs_xFeSe$ (ref. 5), respectively, and their lattice constants determined in this study.

M. If this is the case, it is tempting to conclude that the structure of the high-T_c phase in $(NH_3)_yNa_xFeSe$ may be the same as that of $(NH_3)_yLi_xFeSe$ (or off-center structure, Fig. 4(a)). The suggested structure of the high-T_c phase in $(NH_3)_yNa_xFeSe$ is shown in Fig. 4(b).

On the other hand, the T_c (= 32.5 K) of the low-T_c phase in $(NH_3)_yNa_xFeSe$ may be similar to the T_c (= 31 K) of $(NH_3)_yCs_{0.4}FeSe$, in which the Cs occupies the 2*a* site (0,0,0) (or on-center position) (Fig. 4(d))[5]; our recent Rietveld refinement for XRD of $(NH_3)_yCs_{0.4}FeSe$ showed that the Cs atom occupied 2*a* and N atom in NH_3 occupied 4*c* site. Although the *c* (= 14.145(8) Å) of the low-T_c phase is much smaller than that (= 16.217(1) Å)[5] of $(NH_3)_yCs_{0.4}FeSe$, the difference may be due to the different ionic radius and molecular orientation of NH_3. Consequently, we suggest that the site occupied by the Na atom may be different between the low-T_c and high-T_c phases, *i.e.*, the former involves the on-center positon (Fig. 4(c)), while the latter the off-center position (Fig. 4(b)). This change should be reasonable because of the limited number of sites allowed for Na. Namely, the maximum x allowed for Na in the on-center structure is 0.5, while that in the off-center structure is 1.5. Consequently, when increasing x, $(NH_3)_yNa_xFeSe$ must take the off-center structure. This change probably leads to the different *c*'s that provide the different T_c's.

Very recently, Guo *et al.* showed the presence of non-ammoniated (NH_3-free) $Na_{x'}Fe_2Se_2$ (T_c = 37 K), NH_3-poor $Na_{x'}Fe_2Se_2$ (T_c = 45 K) and NH_3-rich $Na_{x'}Fe_2Se_2$ (T_c = 42 K)[9], and that Na in NH_3-free $Na_{x'}Fe_2Se_2$ occupies the on-center position (called as $ThCr_2Si_2$ structure in Ref. 9). Although they did not report the x dependence of T_c and *c*, it was suggested in their paper that the Coulomb repulsion of Na-Na is an origin for structural destabilization in $(NH_3)_yM_xFeSe$ crystals. We can easily predict that the off-center structure would be more destabilized because of smaller Na-Na distance (nearest Na-Na distance = *a* / 2) than that (nearest Na-Na distance = *a*) of the on-center structure. Nevertheless, because of the limited number of sites for Na, the on-center structure should change to the off-center structure. We suggest that the Coulomb repulsion may be reduced in the off-center structure if the Na atoms select the positions of the 4*c* and 2*b* sites to avoid approaching each other, which would realize the off-center structure in spite of the energetic disadvantage. However, this study still leaves the question open.

Table 1 lists the structural parameters and T_c for the superconducting phases found in this study together with those reported by Guo *et al.*[9] As seen from Table 1, the *c* (= 14.257(7) Å) of the low-T_c phase of $(NH_3)_yNa_{0.28(3)}FeSe$ prepared in this study is larger by ~0.6 Å than that (= 13.6678(4) Å) of the NH_3-free $Na_{x'}Fe_2Se_2$[9] (x' = 2x = 0.65), which suggests that the low-T_c phase contains NH_3 or coordinates between FeSe layers; our data listed in Table 1 correspond to those shown in Fig. 2(d). As described in the **Results** section, the value of y in $(NH_3)_yNa_xFeSe$ was suggested to be 0.2–0.6 for the samples containing the low-T_c phases, suggesting that the $(NH_3)_yNa_xFeSe$ sample showing the T_c of 32 K contains NH_3. The value is close to that, y = 0.3, for the 'NH_3-poor' phase exhibiting the high T_c of 45 K in Guo's

	composition	a (Å)	c (Å)	d (Å)	T_c (K)
low-T_c[a] phase	$(NH_3)_yNa_{0.28(3)}Fe_{0.77(4)}Se$	3.889 (2)	14.257 (7)	7.12	32.5
high-T_c[a] phase	$(NH_3)_yNa_{1.1(1)}Fe_{0.71(3)}Se$	3.8266 (7)	17.565 (9)	8.78	46
NH_3-free[b]	$Na_{0.65(1)}Fe_{1.93(1)}Se_2$	3.7870 (4)	13.6678 (4)	6.83	37
NH_3-poor[b]	$(NH_3)_{0.6}Na0._{80(4)}Fe_{1.86(1)}Se_2$	3.7991 (2)	17.4165 (4)	8.71	45
NH_3-rich[b]	—	—	—	11.1	42

Table 1. Structure and T_c of superconducting phases found for $(NH_3)_yNa_xFeSe$. [a]Taken from this study. The data corresponds to Fig. 2(d). [b]Taken from ref. 9.

paper. As seen from T_c and lattice constants (*a* and *c*) shown in Table 1, our low-T_c phase ($T_c = 32$ K) is different from the NH_3-free phase ($T_c = 37$ K)[9], while our high-T_c phase may be the same as NH_3-poor phase ($T_c = 45$ K)[9]. Thus, $(NH_3)_yNa_xFeSe$ possesses at least four superconducting phases ($T_c = 32.5$, 37, 42 and 45–46 K).

It is significant that the occupancy of Li is fractional at $x < 1.5$ in $(NH_3)_yLi_xFeSe$ (off-center structure), implying that the site occupancy may change continuously in the range $x = 0.1$ to 0.9. Therefore, the continuous variation of *c* (Fig. 3(d)) may be due to this change of occupancy. In other words, changes in the presence and absence of Li at 4*c* and 2*b* sites may be what produce the continuous variation of *c*. In $(NH_3)_yLi_xFeSe$, the presence of some Li at these off-center positions is maintained through the x range of 0.1 to 0.9, in contrast to the progression from on-center to off-center occupancy by Na in $(NH_3)_yNa_xFeSe$. This difference can be attributed to the different ionic radii of Na and Li.

A recent study reported[10] that the T_c *vs.* *c* plot of $(NH_3)_yM_xFeSe$ showed saturated behavior, *i.e.*, T_c increases up to 45 K and then becomes saturated with a monotonic increase in *c*. However, the origin of this saturation behavior[10] is different from that observed in $(NH_3)_yLi_xFeSe$ (Fig. 3(b),(c)) because the *c* does not increase monotonically against x in $(NH_3)_yLi_xFeSe$. Here, we must ask the question why *c* shows a maximum at $x = 0.5$, regardless of the simple prediction that an increase in the amount of Li would cause more expansion of FeSe plane spacing. The local structure around the Li atoms may change depending on x, *i.e.*, the local structure around M (number of NH_3, molecular orientation…) may be different at different x's. At the present stage, we note the possibility that the local structure best able to expand the plane-spacing is realized at $x = 0.5$, although no direct evidence has yet been obtained.

$(NH_3)_yNa_xFeSe$ has more than two different superconducting phases (high-T_c (or NH_3-poor) and low-T_c phases in addition to NH_3-free and NH_3-rich phases[9]), while $(NH_3)_yLi_xFeSe$ has only a single phase with the high T_c. In addition, we recently found that $(NH_3)_yCs_xFeSe$ possessed only a single phase with low T_c (not shown). This is because the Cs metal atom may not occupy off-center positions: the full occupation of those off-center positions would be difficult in view of the larger ionic radius of Cs. Thus, in this paper we conclude that metal occupation is the most significant key to determine the lattice constants and T_c. The influence of amount and molecular orientation of NH_3 should be further investigated. Detailed structural analysis of $(NH_3)_yM_xFeSe$ using the Rietveld refinement of neutron diffraction results is necessary to confirm the exact structure of $(NH_3)_yNa_xFeSe$, which would make the effect of structure (occupation sites) on T_c unequivocal.

Methods

Sample preparation and characterizations. The β-FeSe samples were prepared by the annealing method described in Ref. 6. The samples of $(NH_3)_yM_xFeSe$ (M: Na and Li) were synthesized using the liquid NH_3 technique as described in Ref. 6. All the experimental procedures are the same as in our previous reports[5,8].

The DC magnetic susceptibility, *M* / *H*, of all samples was measured using a SQUID magnetometer (Quantum Design MPMS2); *M* and *H* refer to magnetization and applied magnetic field, respectively. The *M* / *H* in this paper corresponds to mass magnetic susceptibility ($cm^3 g^{-1} = emu\ g^{-1}$). The XRD patterns of the samples were measured with a Rigaku R-AXIS RAPID-NR X-ray diffractometer with Mo *K*α source (wavelength $\lambda = 0.71078$ Å). The samples were introduced into quartz tubes in an Ar-filled glove box for *M* / *H* measurements, while they were introduced into capillaries for XRD. The EDX was measured with an EDX spectrometer equipped with a scanning electron microscope (SEM) (KEYENCE VE-9800 - EDAX Genesis XM_2).

The onset superconducting transition temperature (T_c^{onset}) of all pristine β-FeSe samples prepared in this study was 8.5 K, and the shielding fraction at 2.0 K was ~100%. The XRD patterns of all β-FeSe samples were consistent with each other, and the lattice constants, *a* and *c*, of one β-FeSe sample were determined using LeBail refinement. The lattice constants, *a* (3.77179(4) Å) and *c* (5.5234(1) Å), of the sample were also consistent with published values[5,11,12].

References

1. Ying, T. P. *et al.* Observation of superconductivity at 30–46K in $A_xFe_2Se_2$ (A=Li, Na, Ba, Sr, Ca, Yb, and Eu). *Sci. Rep.* **2,** 426 (2012).
2. Burrard-Lucas, M. *et al.* Enhancement of the superconducting transition temperature of FeSe by intercalation of a molecular spacer layer. *Nature Mater.* **12,** 15–19 (2013).
3. Sedlmaier, S. J. *et al.* Ammonia-rich high-temperature superconducting intercalates of iron selenide revealed through time-resolved *in Situ* X-ray and Neutron diffraction. *J. Am. Chem. Soc.* **136,** 630–633 (2014).
4. Ying, T. P. *et al.* Superconducting Phases in Potassium-Intercalated Iron Selenides. *J. Am. Chem. Soc.* **135,** 2951–2954 (2013).
5. Zheng, L. *et al.* Superconductivity in $(NH_3)_yCs_{0.4}FeSe$. *Phys. Rev. B* **88,** 094521 (2013).
6. Sun, L. L. *et al.* Re-emerging superconductivity at 48 kelvin in iron chalcogenides. *Nature* **483,** 67–69 (2012).
7. Ye, G. J. *et al.* Superconductivity in Yb_xM_yHfNCl (M = NH_3 and THF). *Phys. Rev. B* **86,** 134501 (2012).
8. Sakai, Y. *et al.* Superconducting phases in $(NH_3)_yM_xFeSe_{1-z}Te_z$ (M = Li, Na, and Ca). *Phys. Rev. B* **89,** 144509 (2014).
9. Guo, J. G., Lei, H. C., Hayashi, F. and Hosono, H. Superconductivity and phase instability of NH_3-free Na-intercalated $FeSe_{1-z}S_z$. *Nat. Commun.* **5,** 4756 (2014).
10. Noji T. *et al.* Synthesis and post-annealing effects of alkaline-metal-ethylenediamine-intercalated superconductors $A_x(C_2H_8N_2)yFe_{2-z}Se_2$ (A = Li, Na) with T_c = 45 K. *Physica C* **504,** 8–11 (2014).
11. McQueen T. M. *et al.* Extreme sensitivity of superconductivity to stoichiometry in $Fe_{1+\delta}Se$. *Phys. Rev. B* **79,** 014522 (2009).
12. Hsu F.-C. *et al.* Superconductivity in the PBO-type structure a-FeSe, *Proc. Natl. Acad. Sci.* **105,** 14262–14264 (2008).

Acknowledgments

This study was partly supported by Grants-in-aid (22244045, 24654105, 26105004) from MEXT, by the LEMSUPER project (JST-EU Superconductor Project) of the Japan Science and Technology Agency (JST), and by the Program for Promoting the Enhancement of Research Universities.

Author Contributions

Y.K. (Okayama) designed this research project and supervised experiments. L.Z., X.M., Y.S., M.I. and S.N. synthesized $(NH_3)_yM_xFeSe$ samples, and L.Z. and Y.S. characterized the samples prepared in this study by M / H, XRD and EDX. H.G. and E.U. joined the discussion of this study. The XRD measurement was assisted by Y.K. (Tokyo) and Y.I. Y.K. (Okayama) completed the paper under the discussion with L.Z. and H.G. Y.K. (Okayama) managed all parts of this paper.

Additional Information

Supplementary information accompanies this paper at http://www.nature.com/srep

Competing financial interests: The authors declare no competing financial interests.

How to cite this article: Zheng, L. *et al.* Emergence of Multiple Superconducting Phases in $(NH_3)_yM_xFeSe$ (M: Na and Li). *Sci. Rep.* **5**, 12774; doi: 10.1038/srep12774 (2015).

This work is licensed under a Creative Commons Attribution 4.0 International License. The images or other third party material in this article are included in the article's Creative Commons license, unless indicated otherwise in the credit line; if the material is not included under the Creative Commons license, users will need to obtain permission from the license holder to reproduce the material. To view a copy of this license, visit http://creativecommons.org/licenses/by/4.0/